Molecular BioSystems

Accepted Manuscript

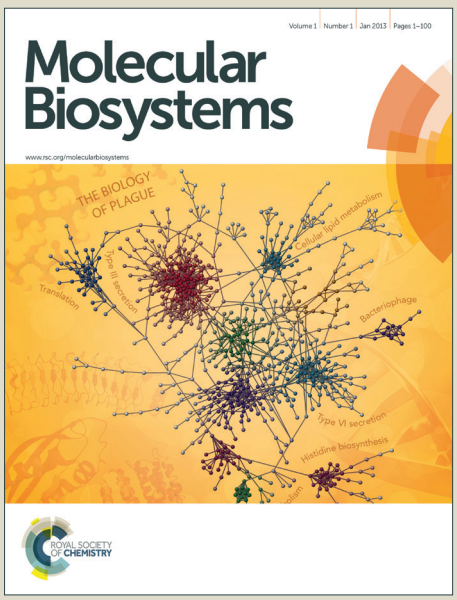

ROYAL SOCIETY OF CHEMISTRY

www.rsc.org/molecularbiosystems

Alterations in rat pulmonary phosphatidylcholines after chronic exposure to ambient fine particulate matter

Wen-Ling Chen[1], Ching-Yu Lin[2], Yuan-Horng Yan[1], Karen T. Cheng[1], Tsun-Jen Cheng[1,*]

[1] Institute of Occupational Health and Industrial Hygiene, College of Public Health, National Taiwan University, No. 17, Xuzhou Rd., Zhongzheng Dist., Taipei City 100, Taiwan

[2] Institute of Environmental Health, College of Public Health, National Taiwan University, Taipei

*Corresponding author

Email addresses:

WLC: d95844001@ntu.edu.tw

CYL: chingyulin@ntu.edu.tw

YHY: r92841010@gmail.com

KTC: karen00102@gmail.com

TJC: tcheng@ntu.edu.tw

Graphical abstract

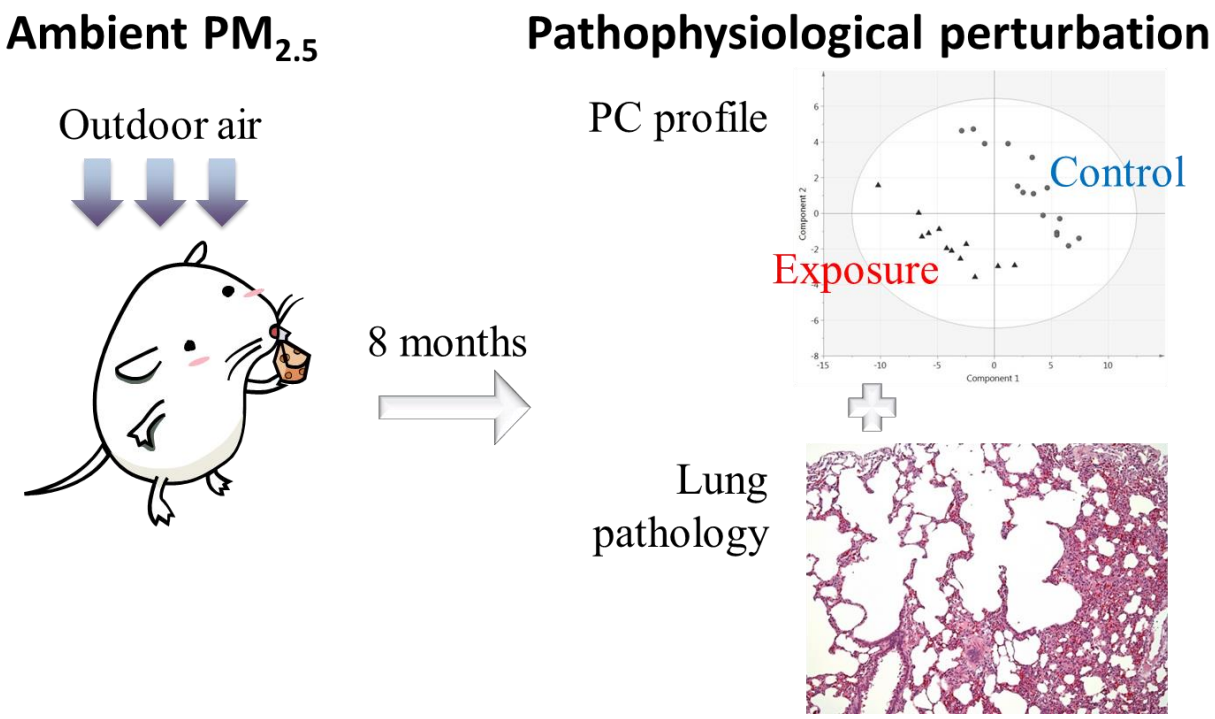

Long-term and low-concentration exposure to ambient $PM_{2.5}$ alters pulmonary phosphatidylcholine profile which conforms to histopathological changes in the lung.

Abstract

This study elucidated the underlying pathophysiological changes that occur after chronic ambient fine particulate matter ($PM_{2.5}$) exposure via a lipidomic approach. Five male Sprague-Dawley rats were continually whole-body exposed to ambient air containing $PM_{2.5}$ at 16.7 ± 10.1 μg/m^3 from the outside of the building for 8 months, whereas a control group (n = 5) inhaled filtered air. Phosphorylcholine-containing lipids were extracted from lung tissue and profiled using ultraperformance liquid chromatography-tandem mass spectrometry (UPLC-MS/MS). The phosphatidylcholine (PC) signal features of the two groups were compared using partial least squares discriminant analysis (PLS-DA) and Wilcoxon rank sum tests. The PC profile of the exposure group differed from that of the control group; the R^2Y and Q^2 were 0.953 and 0.677, respectively, in the PLS-DA model. In the exposure group, a significant 0.66- to 0.80-fold reduction in lyso-PC levels, which may have resulted from repeated inflammation, was observed. Decreased surfactant PCs by 16% at most may indicate injuries to alveolar type II cells. Cell function and cell signalling are likely to be altered because the decrease in unsaturated PCs may reduce membrane fluidity. Accompanied by the decline in plasmenylcholines, decreased unsaturated PCs may indicate the attack of reactive oxygen species generated by $PM_{2.5}$ exposure. The physiological findings conformed to the histopathological changes in the exposed animals. PC profiling using UPLC-MS/MS-based lipidomics is sensitive for reflecting pathophysiological perturbations in the lung after long-term and low concentration $PM_{2.5}$ exposure.

Keywords: Ambient fine particulate matter ($PM_{2.5}$), Long-term exposure, Lipidomics, Phosphatidylcholine profile, Ultraperformance liquid chromatography tandem mass spectrometry (UPLC-MS/MS)

1. Introduction

Numerous epidemiological studies have linked exposure to ambient fine particulate matter ($PM_{2.5}$, < 2.5 μm in aerodynamic diameter) with pulmonary and cardiovascular effects, such as exacerbation of symptoms, increased hospital admission, and increases in mortality caused by asthma, lung cancer, and chronic obstructive pulmonary disease [1-4]. In addition, one study observed a dose-response relationship between long-term exposure and the relative risks of death related to pulmonary, cardiovascular, and cardiopulmonary causes [5].

Inflammatory reactions might be essential to ambient- $PM_{2.5}$-induced pulmonary and cardiovascular effects. Inconsistent trends have been observed in inflammatory biomarkers after ambient $PM_{2.5}$ exposure, including increased levels of cytokines such as macrophage inflammatory protein-2 and tumour necrosis factor-α (TNF-α), decreased Clara-cell secretory protein-16 levels, and unchanged interleukin-6 (IL-6) levels in biofluids, and may indicate possible but slight inflammatory responses [6, 7]. In the human alveolar cell line A549, urban ambient $PM_{2.5}$ induced the release of proinflammatory cytokines IL-6 and IL-8, reduced cell survival, and increased cell apoptosis [8], whereas, in human alveolar macrophages, exposure to 100 μg/mL of ambient $PM_{2.5}$ caused the release of TNF-α to be suppressed by 38.7% [9]. In addition to inflammation, $PM_{2.5}$ exposure may cause elevated oxidative stress by generating reactive oxygen or nitrogen species in the cardiopulmonary system [10, 11]. Despite numerous studies on the health effects of ambient $PM_{2.5}$, the mechanism of lung injury caused by long-term and low-concentration exposure is unclear. Moreover, traditional biomarkers for acute responses, such as inflammation, may fail to indicate chronic effects, particularly among organisms that have adapted and developed tolerance after such exposure. Therefore, novel approaches that enable more sensitive detection of pathophysiological perturbations are required.

Metabolomics involves studying the entire profile of small molecules, primarily endogenous molecules associated with specific physiological status in cells, enabling toxicological mechanisms

to be understood thoroughly [12, 13]. In one study, mice with asthma exhibited an altered metabolome, including the metabolites associated with energy, sterols, and lipid metabolism, as well as carbohydrates [14]. Lipidomics involves profiling lipids and has been applied in several respiratory studies. For example, low- and very-low-density lipoprotein concentrations in the serum were higher in asthma patients with low forced expiratory volume in one second compared with other patients [15]. Changes in phospholipids are of great concern because of the abundance and importance of phospholipids in cells. Phospholipid profiling has been applied to identifying the biomarkers and elucidating toxicological mechanisms of certain exposures, symptoms, and diseases [16-18]. Regarding exposure, phospholipid oxidation in the lungs was associated with exposure to nanomaterials [19]. Cigarette smoking may reduce some cholesteryl esters, phosphatidylcholine (PC)(18:0/20:4), and lyso-PC(20:4) in plasma despite the overall increase in plasma lipids [20]. Regarding health effects, changes in PCs and phosphatidylethanolamines in biofluids or tissues have been linked to hypertension, diabetes, cardiovascular diseases, and cancer [21, 22].

PC is a glycerophospholipid containing a choline head group esterified at *sn-3* position and fatty acyl (FA) chains consisting of 12 to 26 carbons and up to six unsaturated double bonds on either *sn-1 or 2* position [22]. PC accounts for 70%–80% of phospholipids and, consequently, plays a critical role in cell integrity and cell signalling [23, 24]. It is a major component of surfactants and, thus, a reduction in PC may cause abnormal surfactant functions, which are highly relevant to pulmonary toxicity. In addition, saturation on the FA chains in PCs is associated with low fluidity and high rigidity of cell membranes. For example, respiratory distress syndrome (RDS) results from immaturity of the lungs, affecting primarily the surfactant synthesising system. In infants with RDS, the number of PCs consisting of unsaturated FA chains is low, causing the surfactant monolayer to be unstable and reduction of surface tension to fail [23]. In addition, the decrease in PCs is associated with acute and chronic respiratory diseases in adults such as pneumonia and chronic obstructive lung disease, respectively [24]. A decrease in total PC was observed in asthma mice, and after dexamethasone treatment, lyso-PC synthesis was upregulated [14]. PC(32:3), PC(34:1), PC(36:3), and

PC(36:2) concentrations were higher in human lung cancer tissues, including tumour and biopsy samples, compared to normal tissues [25]. A significant discrimination in PC profiles containing decreased lyso-PCs, PC(16:0/0:0), PC(18:0/0:0), PC(18:1/0:0), and PC(18:2/0:0) in patients with lung cancer was also reported [26].

Nuclear magnetic resonance can be used to detect phospholipids, but not to distinguish and quantify lipids of different structures due to its low resolution unless taking hours to analyse one sample in order to achieve satisfying resolution; thus, nuclear magnetic resonance provides limited information on lipids. High-throughput liquid chromatography–tandem mass spectrometry (LC-MS/MS) methods that involve pretreatments entailing liquid–liquid extraction conducted using methanol and chloroform are increasingly applied in lipidomics. These methods enable PC subclasses, which have discerned features and roles in various metabolism pathways, to be profiled and used to describe pathophysiological statuses in detail [21, 22, 27-29]. In this study, we demonstrated the underlying pathophysiological changes in Sprague-Dawley rats that were chronically exposed to ambient $PM_{2.5}$ by applying ultraperformance LC-MS/MS (UPLC-MS/MS)-based lipidomics developed by Tang et al. [28].

2. Methods

2.1. Animal study design

All the animal study conducted in this study was approved according to the Institutional Animal Care and Use Committee of the National Taiwan University College of Medicine and the College of Public Health (Approval No. 20120254).

Ten male Sprague-Dawley rats aged 6 weeks were purchased from Lasco, Charles River Technology (Yilan, Taiwan) and acclimated for 14 days before the experiment was conducted. They had free access to rodent chow and water. The average body weight before exposure and at necropsy was 375 g and 749 g, respectively. The rat dwelled in Individually Ventilated Cages (Tecniplast Inc., Exton, PA, USA) modified for continual, whole-body exposure to ambient air. The cages were located at the Inhalation Toxicology Laboratory in National Taiwan University College of Public Health Building in downtown Taipei City. Each cage was connected individually to an air handling unit to ensure homogeneous distribution of the air. The non-filtered, non-concentrated air delivered by the air handling unit was drawn directly from the outside of the laboratory through an inlet installed on a window faced south at a flow rate of 79 ± 1.0 m^3/hour (mean ± standard deviation). The particle loss during air introduction was 18-21%, which was estimated by comparing the outside and in-cage $PM_{2.5}$ concentrations measured using a P-Track particle counter (TSI Inc., Minneapolis, MN, USA) during the experiment. The particle loss may have resulted from diffusion, deposition, and sedimentation at the tubing, the blower, and manifold racks. Besides, the mass concentration measured using a dust monitor (DUST-check, model 1.108; Grimm Labortechnik Ltd., Ainring, Germany) revealed that the fine particles accounted for 99.2-99.9% of total PM less than 10 μm in diameter (PM_{10}) in the cage, which demonstrated removal of coarse particles and preservation of the majority of $PM_{2.5}$ by this whole system. The gas-phase pollutants were directed without treatment into the cage.

While the exposure group (n = 5) exposed to ambient air, the control group (n = 5) inhaled filtered air flowing through a high-efficiency particulate air purifier added on the inlet valve. The gas-phase pollutants were evenly distributed in the cage of each group. The concentrations of $PM_{2.5}$ in the exposure and control cages throughout the experiment were 16.7 ± 10.1 μg/m^3 and 0.70 ± 0.46 μg/m^3 (mean ± standard deviation), respectively. The soluble ions in the particles were predominated by organic carbon (30.9%) and sulfate (30.4%), followed by ammonium (14.8%) and nitrate (11.4%), which represented typical traffic-related air pollution in the area. The experiment lasted from November 2012 to June 2013.

Rats were sacrificed using overdosed Zoletil (Virbac, Carros, France). Blood were collected through the direct withdrawal from the abdominal aorta. After animals' scarification, punctured lungs were filled with 4% formaldehyde and knotted. The entire lung tissue was immersed in the 4% formaldehyde for overnight. Tissue samples were cleared in xylene and embedded in paraffin wax. Serial sections (5μm thickness) were sliced followed by hematoxylin and eosin staining. Sections were examined under light microscope.

2.2. Sampling and analysis of phosphatidylcholines

The right-lobe of the lungs was resected, wrapped in aluminium foil, and snap-frozen with liquid nitrogen. Immediately before lipid extraction, the lung tissue was homogenised using a mortar and a pestle at a low temperature in liquid nitrogen. The homogenised tissue was freeze-dried using a ScanVac lyophiliser (LaboGene, Lynge, Denmark). We extracted the phospholipids from the dried tissue by applying the method developed by Folch et al. [30]. Briefly, 1-mg lung tissue was spiked with the internal standard of 1.0 μg/mL of sphingomyelin (d18:1/17:0) in 0.2 mL of methanol. After thorough vortexing the spiked tissue, we added 0.15 mL of 0.15 M sodium chloride$_{(aq)}$ and 0.4 mL of chloroform, sequentially, to it. The mixture was vortexed for 10 min and centrifuged for 10 min at 10,000 rpm and 4 ℃. Subsequently, 0.4 mL of the lower layer was

removed and dried, and then reconstituted with 0.2 mL of methanol. After filtered, the sample was ready for instrumental analysis.

According to the procedure described by Tang et al. [28], three duplicate PC analyses were examined by using a Waters ACQUITY UPLC coupled with a Quattro Premier XE (Waters, Milford, MA, USA) UPLC-MS/MS. The PCs were separated using a BEH C_{18} column (1.7 μm, 2.1 mm × 100 mm, Waters, Milford, MA, USA) at a flow rate of 0.7 mL/min and a temperature of 70 ℃. The mobile phases were (A) 10 mM ammonium acetate$_{(aq)}$ and (B) acetonitrile–methanol (65:35, v/v) with 10 mM of ammonium acetate. The LC gradient began from 55% B, climbed to 70% in 0.1 min, increased to 100% in 1.4 min, and remained at 100% for 4.5 min. The column was then reequilibrated with 45% A and 55% B. The total chromatographic time was 10 min. For MS detection, we used electrospray ionisation and scanned the PC precursor ions of the positive ion of mass-to-charge ratio *(m/z)* at 184, which is the protonated $[M + H]^+$ ion of the phosphocholine head group. The capillary charge was set at 2.5 kV. The temperatures applied for ionisation and desolvation were 120 ℃ and 450 ℃, respectively. The flow rate of the cone gas was 50 L/h, and that for desolvation was 700 L/h. The cone voltage and collision energy were set at 35 V and 30 V, respectively.

2.3. Chemometrics

The chromatograms were analysed using MZmine 2.10 [31]. We developed the chromatograms by using a minimal signal intensity of 3000 and an *m/z* tolerance of 1000 ppm; a maximal number of 110 lipid features for a sample were confirmed. The peak area of each lipid was normalised to the total peak area of a chromatogram. Normalised data were analysed using multivariate analyses encoded within SIMCA 13.0.3 (Umetrics, Umeå, Sweden). After logarithm transformation and univariance scaling, we performed principal component analysis (PCA), an unsupervised method, to visualize the clustering of samples. Partial least squares discriminant analysis (PLS-DA) was subsequently performed to learn the primary PCs attributing to the profile differences between the

exposure and the control group. The PLS-DA model was evaluated using R^2Y and Q^2. R^2Y denotes the degree to which the components describe the central tendency. Q^2 is calculated based on the sum of error between the predicted and the experimental central tendency [32, 33]. In addition, we performed a permutation test which involved randomly assigning a considerable number of samples (500 in this study) to the two groups. If all of the 500 Q^2 levels in the randomly grouped models were lower than those in the experimental model, the experimental model is diagnosed statistically significant. The variable importance in projection (VIP) score of each PC indicated the importance of the PC and was calculated based on its loading weights [34]. One outlier in the PLS-DA model in the exposure group was excluded. This sample failed to be completely dried after lyophilisation, and its overall signal intensity was approximately 10 times lower than that of other samples because of probable PC degradation.

The folds of changes of PCs were calculated by the average peak area ratio of a PC in the exposure group to the control group. The differences between the normalised peak areas in the two groups were tested for significance using Wilcoxon rank sum tests. We identified the PCs and plasmenylcholines that had p values lower than 0.05 according to the Wilcoxon rank sum tests administered to compare the two groups and VIP scores higher than 1.00 in the PLS-DA model. We matched the *m/z* and retention time using the in-house library established by Tang et al. [28]. For the lipids that were not listed in the library, we compared the *m/z* with those in the LIPID Metabolites and Pathways Strategy (LIPID MAPS) structure database to obtain information on their total numbers of carbons and unsaturated double bonds in the FA chains and were expressed as PC(carbon number:double bond number) [35].

3. Results and Discussion

3.1. Histopathology

After 8 months of exposure, there were no observable disease symptoms except low activity caused by ageing and obesity (data not shown). Histopathology revealed the lung has differences between the exposure and control group (Figure 1). We observed an obviously enlarged alveolar size and reduced alveolar number in the exposure group, confirming that emphysema caused by pulmonary injuries developed in all of the exposed animals. By contrast, the alveoli in the control group were generally within the normal range, although some minor emphysema and arteriole thickening, which could be attributed to aging, was observed. In addition to emphysema, the exposed animals exhibited sporadic petechiae and congestion on the alveoli and thickened tunica media on pulmonary arterioles in the exposed animals. Increased inflammatory cells were also observed in the exposure group (Figure 2).

3.2. Phosphatidylcholine profile

A total of 110 phosphorylcholine-containing lipids were separated and detected in the lung tissue. The PC profile of the exposed animals (n = 4) differed from that in the control group (n = 5) in that the R^2Y and Q^2 were 0.953 and 0.677, respectively, in the PLS-DA model (Figure 3). The model satisfied the permutation test. Forty-one phosphorylcholine-containing lipids yielded VIP scores higher than 1.0 in the PLS-DA model. Twenty-five differed significantly between the exposure and the control group ($p < 0.05$) according to Wilcoxon rank sum tests conducted to compare the two groups. Only PCs and plasmenylcholines that fulfilled the VIP and p value criteria were listed in Table 1. We analysed the trends in these PCs, including three lyso-PCs, two surfactant PCs, six PCs consisting of polyunsaturated fatty acyl (PUFA) chains, and four plasmenylcholines to describe the pathophysiological changes in the lung.

3.3. Lysophosphatidylcholine

The levels of lyso-PCs, PC(16:0/0:0), PC(18:1/0:0), and PC(18:0/0:0) were 0.66- to 0.80-fold lower in the rats exposed to ambient $PM_{2.5}$ compared with the control group (Table 1). The decrease in lyso-PCs could have resulted from abnormal phospholipase activity and may indicate inflammation. Phospholipase A_2 (PLA_2) catalyses the major generation form of lyso-PCs in the lungs that originate from the polar surface PCs of lipoproteins or from PCs in cell membranes [36].

Inflammatory responses can be accompanied by decreases in lyso-PCs through several pathways. Ried et al. [32] observed a negative association between lyso-PCs consisting of 16 to 18 carbons on the FA chain and current asthma and attributed this to a chronic, low-grade inflammatory state with altered composition of lipids as well as abnormal lipid and lipoprotein metabolism. Lyso-PCs can be depleted to participate in eosinophil infiltration, thus promoting inflammation and increasing respiratory resistance [37]. Furthermore, lyso-PCs can reduce proinflammatory cytokines in relation to TNF-α, and the decrease in lyso-PCs might indicate a low potential for preventing inflammation [38]. The result obtained in this study regarding lyso-PCs was consistent with previous findings on asthma. In addition, we confirmed the increase in inflammatory cells in the exposed group according to pulmonary histopathology (Figure 2).

Changes in pulmonary lyso-PCs may also indicate perturbations in cell function and cell signalling [39], imposing additional stresses on the lung. In rats exhibiting decreased lyso-PCs caused by pharmacological castration, the lung morphology revealed altered parenchyma, numerous macrophages, fibrosis, and large empty spaces caused by rupture of the interalveolar septa [40]. Among lung cancer patients, decreased PC(16:0/0:0), PC(0:0/16:0), PC(18:0/0:0), and PC(18:1/0:0) levels were attributed to cell proliferation, a high metabolic state, and abnormal expression of acyl CoA:lysophosphatidylcholine acyltransferase 1 ($LPCAT_1$), which remodels lyso-PCs [26]. The septa breaks that we observed may have resulted partially from the decrease in lyso-PCs rather than severe pathological changes, such as carcinoma.

3.4. Surfactant phosphatidylcholine

A 86% and 84% lower abundance of surfactant PCs, PC(16:0/20:4) and PC(18:0/18:1), respectively, was found in the lung tissue in the exposure group compared with the control group (Table 1). In addition, a 7% lower and a 13% higher abundance of dipalmitoylphosphatidylcholine (DPPC, PC(16:0/16:0) and its precursor, PC(34:1), respectively, were observed in that the VIP score was higher than 1.00, although the Wilcoxon rank sum tests implied insignificant differences. DPPC is a major surfactant PC in the pulmonary surfactant system and accounts for 60.6% of the total PCs in the human surfactant [41]. DPPC is synthesised by two mechanisms. Remodelling from PC(34:1) is a major mechanism to generate DPPC, whereas a de novo pathway is attributed to less than 50% of DPPC generation. Remodelling consists of two steps. First, PC(16:0/18:1) produces the lyso-PC, PC(16:0/0:0), through PLA_2-catalysed deacylation. Second, $LPCAT_1$ catalyses the reacylation and palmitation of PC(16:0/0:0) into DPPC. The secreted surfactants are then packed into lamellar bodies, transformed into tubular myelin, and finally form the monolayer film at the air-fluid interface to maintain low surface tension on the alveoli [24, 27]. A mild normal stretch of the alveolar type II cell activates PLA_2 and $LPCAT_1$, causing a rapid increase in the DPPC proportion in PCs [42]. In this study, the increase in PC(34:1) and decreases in surfactant PCs indicated precursor molecule accumulation and difficulty in forming the surfactant, which may have resulted from alveolar type II cell damage.

Particle exposure may damage alveolar epithelial type II cells and restrict their mechanical stretching, signifying dysfunctions in surfactant PC synthesis. The shortage of pulmonary surfactants can cause alveolar surface tension to increase and the gas–liquid interface to become disorganised, resulting in damage to the monolayer, septa breaks, and fusion of alveolar cavities [40, 41]. The pathological mechanism was consistent with the findings of this study regarding both the surfactant PC reduction and morphological observation in that several alveolar cavities fused into one, lowering the alveolar number and enlarging the average size [43]. In addition, previous studies on surfactant protein-D null mice have indicated that pulmonary phospholipid accumulation, impaired

pulmonary PC catabolism, and low surfactant PC secretion are correlated with the emphysema development [44, 45]. However, the established emphysema can cause surfactant PCs to be reduced, enabling an increase in surface tension, which is a compensation mechanism for maintaining recoil pressure that enables sufficient alveolar compression after expansion [46]. Although whether the decrease in surfactant PCs in this study was an effect of alveolar type II cell damage or preexisting emphysema is not concluded, surfactant PCs were evident indicators of emphysema-like pathological changes (Figure 1) after chronic exposure to $PM_{2.5}$ at an environmentally relevant concentration.

3.5. Phosphatidylcholine with polyunsaturated fatty acyl chains

Significant decreases in 6 PCs consisting of long PUFA chains, which contained at least 34 carbons and more than 3 unsaturated bonds, were observed in the exposure group (Table 1). This result is partially consistent with the finding reported by Boué et al. [20], who observed that cigarette smoke lowers the levels of PCs consisting of PUFA chains in mice.

The unsaturated double bonds in the FA chains can improve cell integrity by maintaining membrane completion. Each unsaturated bond forms a rigid kink on the long FA chain. The kinks render the chain less twistable and the chemical structure stiffer compared with a saturated chain. When additional PCs consisting of PUFA chains form a phospholipid bilayer, the cell membrane is firm and less likely to break because of external forces [47]. In addition, additional PUFA chains may influence cell function. The kinks formed by unsaturated bonds shape space that biomolecules can permeate easily. The enhanced membrane fluidity can thus affect the functions in which these biomolecules are involved [47]. Li and Yuan [36] reported that, after paclitaxel treatment in the cervical cancer cell line HeLa, the number of PCs consisting of PUFA chains decreased and the chain lengths shortened. These outcomes may collectively cause poor membrane fluidity and, consequently, alter the mobility and functions of biomolecules, such as proteins on the membrane,

ultimately affecting cell apoptosis. The decrease in PCs consisting of PUFA chains in this study may indicate that ambient $PM_{2.5}$ is likely to alter cell integrity and cell functions in the lung tissue.

The unsaturated bonds in FA chains have also been proved to protect the membranes from attack by hydroxyl radicals. These unsaturated bonds reinforce lipid peroxidation to depress the hydroxyl radical levels, retarding the hydroxyl radical actions to alter other molecules on the membrane, preventing changes in membrane constituents [48]. In addition, respiratory oxidative burst can be inhibited through a mechanism in which PCs consisting of long PUFA chains diminish the oxidative stress in neutrophils by inhibiting protein kinase C instead of reducing superoxides [49]. Previous studies have confirmed that fine particle exposure generates reactive oxygen species (ROS) [50-54]. The rises in ROS may be attributed to the decrease in PCs consisting of long PUFA chains observed in this study. This observation was consistent with the declines in plasmenylcholines because the vinyl ether bond is susceptible to ROS attack [55].

4. Conclusions

LC-MS/MS-based lipidomics demonstrated alterations in the PC profiles of the lung tissue of Sprague-Dawley rats that were chronically exposed to ambient $PM_{2.5}$. The decreases in lyso-PCs, surfactant PCs, PCs consisting of long PUFA chains, and plasmenylcholines may indicate pathophysiological changes in the lungs, including ongoing inflammatory responses, damages of alveolar sacks, altered cell integrity, and affected cell functions after PM exposure. Pulmonary injury was validated based on the presence of emphysema in the lung histopathology. LC-MS/MS-based PC profiling is a sensitive method for examining pathophysiological perturbations which enables gaining insight the underlying mechanisms of pulmonary injury induced by long-term and low-concentration $PM_{2.5}$ exposure at the cellular level.

Acknowledgements

The authors would like to acknowledge the financial support provided by the Taiwan Ministry of Science and Technology (NSC 101-2314-B-002-116-MY2).

References

1. J. I. Halonen, T. Lanki, T. Yli-Tuomi, M. Kulmala, P. Tiittanen and J. Pekkanen, *Thorax*, 2008, **63**, 635-641.
2. A. Wheeler, A. Zanobetti, D. R. Gold, J. Schwartz, P. Stone and H. H. Suh, *Environ. Health Persp.*, 2006, **114**, 560-566.
3. K. L. Jansen, T. V. Larson, J. Q. Koenig, T. F. Mar, C. Fields, J. Stewart and M. Lippmann, *Environ. Health Persp.*, 2005, **113**, 1741-1746.
4. K. Katanoda, T. Sobue, H. Satoh, K. Tajima, T. Suzuki, H. Nakatsuka, T. Takezaki, T. Nakayama, H. Nitta, K. Tanabe, S. Tominaga and G. Three-Prefecture Cohort Study, *J. Epidemiol.*, 2011, **21**, 132-143.
5. A. D. Kappos, P. Bruckmann, T. Eikmann, N. Englert, U. Heinrich, P. Hoppe, E. Koch, G. H. M. Krause, W. G. Kreyling, K. Rauchfuss, P. Rombout, V. Schulz-Klemp, W. R. Thiel and H. E. Wichmann, *Int. J. Hyg. Envir. Heal.*, 2004, **207**, 399-407.
6. B. Behbod, B. Urch, M. Speck, J. A. Scott, L. Liu, R. Poon, B. Coull, J. Schwartz, P. Koutrakis, F. Silverman and D. R. Gold, *Occup. Environ. Med.*, 2013, **70**, 761-767.
7. T. Halatek, M. Stepnik, J. Stetkiewicz, A. Krajnow, B. Kur, W. Szymczak, K. Rydzynski, E. Dybing and F. R. Cassee, *J. Environ. Sci. Heal. A*, 2011, **46**, 1469-1481.
8. R. B. Hetland, F. R. Cassee, M. Refsnes, P. E. Schwarze, M. Lag, A. J. F. Boere and E. Dybing, *Toxicol. in Vitro*, 2004, **18**, 203-212.
9. K. Sawyer, S. Mundandhara, A. J. Ghio and M. C. Madden, *Journal of Toxicology and Environmental Health-Part a-Current Issues*, 2010, **73**, 41-57.
10. P. Gillespie, J. Tajuba, M. Lippmann, L.-C. Chen and B. Veronesi, *Neurotoxicology*, 2013, **36**, 112-117.
11. R. Miyata and S. F. van Eeden, *Toxicol. Appl. Pharm.*, 2011, **257**, 209-226.
12. S. G. Oliver, M. K. Winson, D. B. Kell and F. Baganz, *Trends Biotechnol.*, 1998, **16**, 373-378.

13. R. Goodacre, S. Vaidyanathan, W. B. Dunn, G. G. Harrigan and D. B. Kell, *Trends Biotechnol.*, 2004, **22**, 245-252.

14. W. E. Ho, Y.-J. Xu, F. Xu, C. Cheng, H. Y. Peh, S. R. Tannenbaum, W. S. F. Wong and C. N. Ong, *Am. J. Resp. Cell Mol.*, 2013, **48**, 204-211.

15. J. Jung, S. H. Kim, H. S. Lee, G. S. Choi, Y. S. Jung, D. H. Ryu, H. S. Park and G. S. Hwang, *Clin. Exp. Allergy*, 2013, **43**, 425-433.

16. P. Bougnoux, N. Hajjaji and C. Couet, *Prostag. Leukotr. Ess.*, 2008, **79**, 93-96.

17. J. J. Kamphorst, J. R. Cross, J. Fan, E. de Stanchina, R. Mathew, E. P. White, C. B. Thompson and J. D. Rabinowitz, *P. Natl. Acad. Sci. USA*, 2013, **110**, 8882-8887.

18. C.-H. Tang, C.-Y. Lin, S.-H. Lee and W.-H. Wang, *Aquat. Toxicol.*, 2014, **148**, 1-8.

19. Y. Y. Tyurina, E. R. Kisin, A. Murray, V. A. Tyurin, V. I. Kapralova, L. J. Sparvero, A. A. Amoscato, A. K. Samhan-Arias, L. Swedin, R. Lahesmaa, B. Fadeel, A. A. Shvedova and V. E. Kagan, *ACS Nano*, 2011, **5**, 7342-7353.

20. S. Boue, K. Tarasov, M. Janis, S. Lebrun, R. Hurme, W. Schlage, M. Lietz, G. Vuillaume, K. Ekroos, Y. Steffen, M. C. Peitsch, R. Laaksonen and J. Hoeng, *Atherosclerosis*, 2012, **225**, 328-334.

21. J. Ecker, *J. Sep. Sci.*, 2012, **35**, 1227-1235.

22. U. Loizides-Mangold, *Febs J.*, 2013, **280**, 2817-2829.

23. A. Greenough and V. Murthy, *Fetal and Maternal Medicine Review*, 2008, **19**, 203-225.

24. M. Agassandian and R. K. Mallampalli, *BBA-Mol. Cell Biol. L.*, 2013, **1831**, 612-625.

25. G. K. Lee, H. S. Lee, Y. S. Park, J. H. Lee, S. C. Lee, J. H. Lee, S. J. Lee, S. R. Shanta, H. M. Park, H. R. Kim, I. H. Kim, Y. H. Kim, J. I. Zo, K. P. Kim and H. K. Kim, *Lung Cancer*, 2012, **76**, 197-203.

26. J. Dong, X. Cai, L. Zhao, X. Xue, L. Zou, X. Zhang and X. Liang, *Metabolomics*, 2010, **6**, 478-488.

27. G. Schmitz and K. Ruebsaamen, *Atherosclerosis*, 2010, **208**, 10-18.

28. C.-H. Tang, P.-N. Tsao, C.-Y. Chen, M.-S. Shiao, W.-H. Wang and C.-Y. Lin, *J. Chromatogr. B*, 2011, **879**, 2095-2106.

29. C.-H. Tang, P.-N. Tsao, C.-Y. Lin, L.-S. Fang, S.-H. Lee and W.-H. Wang, *Anal. Bioanal. Chem.*, 2012, **404**, 2949-2961.

30. J. Folch, M. Lees and G. H. S. Stanley, *J. Biol. Chem.*, 1957, **226**, 497-509.

31. T. Pluskal, S. Castillo, A. Villar-Briones and M. Orešič, *BMC bioinformatics*, 2010, **11**, 395.

32. E. Szymanska, E. Saccenti, A. K. Smilde and J. A. Westerhuis, *Metabolomics*, 2012, **8**, 3-16.

33. B. Worley and R. Powers, *Current Metabolomics*, 2013, **1**, 92-107.

34. S. Wold, M. Sjöström and L. Eriksson, *Chemometr. Intell. Lab.*, 2001, **58**, 109-130.

35. M. Sud, E. Fahy, D. Cotter, A. Brown, E. Dennis, C. Glass, R. Murphy, C. Raetz, D. Russell and S. Subramaniam, *Nucleic Acids Res.*, 2006, **35**, D527-532.

36. X. Li and Y.-J. Yuan, *Omics*, 2011, **15**, 655-664.

37. O. Nishiyama, H. Kume, M. Kondo, K. Ito, M. Ito and K. Yamaki, *Clin. Exp. Pharmacol. Physiol.*, 2004, **31**, 179-184.

38. G. Murugesan, M. R. S. Rani, C. E. Gerber, C. Mukhopadhyay, R. M. Ransohoff, G. M. Chisolm and K. Kottke-Marchant, *J. Mol. Cell Cardiol.*, 2003, **35**, 1375-1384.

39. A. Tokumura, *J. Health Sci.*, 2011, **57**, 115-128.

40. M. S. Ojeda, N. N. Gomez, E. Gil, L. Scardapane and M. S. Gimenez, *Braz. J. Med. Biol. Res.*, 2000, **33**, 279-285.

41. A. Dushianthan, R. Cusack, V. Goss, A. D. Postle and M. P. W. Grocott, *Crit. Care*, 2012, **16**.

42. D. Pantazi, E. Kitsiouli, A. Karkabounas, T. Trangas, G. Nakos and M. E. Lekka, *Lipids*, 2013, **48**, 827-838.

43. L. Knudsen, M. Ochs, R. MacKay, P. Townsend, R. Deb, C. Muehlfeld, J. Richter, F. Gilbert, S. Hawgood, K. Reid and H. Clark, *Resp. Res.*, 2007, **8**.

44. L. Q. Zhang, M. Ikegami, E. C. Crouch, T. R. Korfhagen and J. A. Whitsett, *Journal of Biological Chemistry*, 2001, **276**, 19214-19219.

45. L. Q. Zhang, M. Ikegami, C. R. Dey, T. R. Korfhagen and J. A. Whitsett, *J. Biol. Chem.*, 2002, **277**, 38709-38713.

46. E. P. Ingenito, L. W. Tsai, A. Majumdar and B. Suki, *Am. J. Respir. Crit. Care Med.*, 2005, **171**, 300-304.

47. J. E. Darnell, H. F. Lodish and D. Baltimore, *Molecular cell biology*, Distributed by W.H. Freeman, New York, 1990.

48. C. Barth and G. Stark, *Biochimica Et Biophysica Acta*, 1991, **1066**, 54-58.

49. K. Yoshida and V. Mohsenin, *Life Sci.*, 1991, **49**, 1359-1365.

50. S. A. Weichenthal, K. Godri-Pollitt and P. J. Villeneuve, *Environ. Health*, 2013, **12**.

51. F. Tao, B. Gonzalez-Flecha and L. Kobzik, *Free Radic. Biol. Med.*, 2003, **35**, 327-340.

52. T. D. Nelin, A. M. Joseph, M. W. Gorr and L. E. Wold, *Toxicol. Lett.*, 2012, **208**, 293-299.

53. N. Li, M. Q. Hao, R. F. Phalen, W. C. Hinds and A. E. Nel, *Clin. Immunol.*, 2003, **109**, 250-265.

54. Y. Kumagai and N. Shimojo, *J. Health Sci.*, 2001, **47**, 439-445.

55. K. Gorgas, A. Teigler, D. Komljenovic and W. Just, *Biochim. Biophys. Acta*, 2006, **1763,** 1511-1526.

Figures

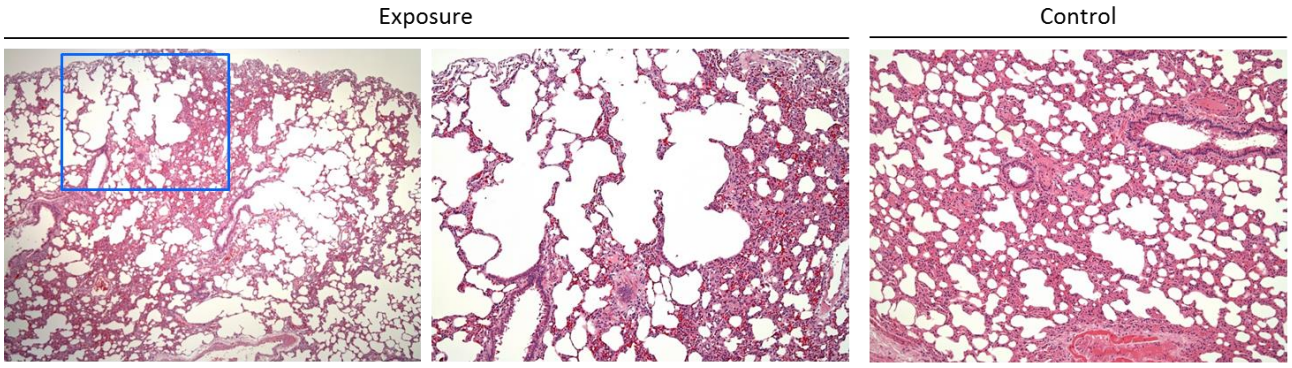

	1-1	*1-2*	*1-3*	*1-4*	*1-5*	*2-1*	*2-2*	*2-3*	*2-4*	*2-5*
Emphysema, alveolar	**2**	**2**	**2**	**2**	**2**	**1**		**1**	**1**	**1**
Petechiae and congestion, alveolar, focal	**1**		**1**							
Tunica media thickening, pulmonary arterioles				**1**	**1**				**1**	
Tunica media mineralization, pulmonary arterioles									**1**	

1-1 —*1-5*: Exposure group; *2-1* —*2-5*: Control group
Score **1**: minimal
Score **2**: slight

Figure 1 Lung morphology revealed emphysematous change in Sprague-Dawley rats exposed to ambient $PM_{2.5}$ while the alveoli in the control group was normal in general.

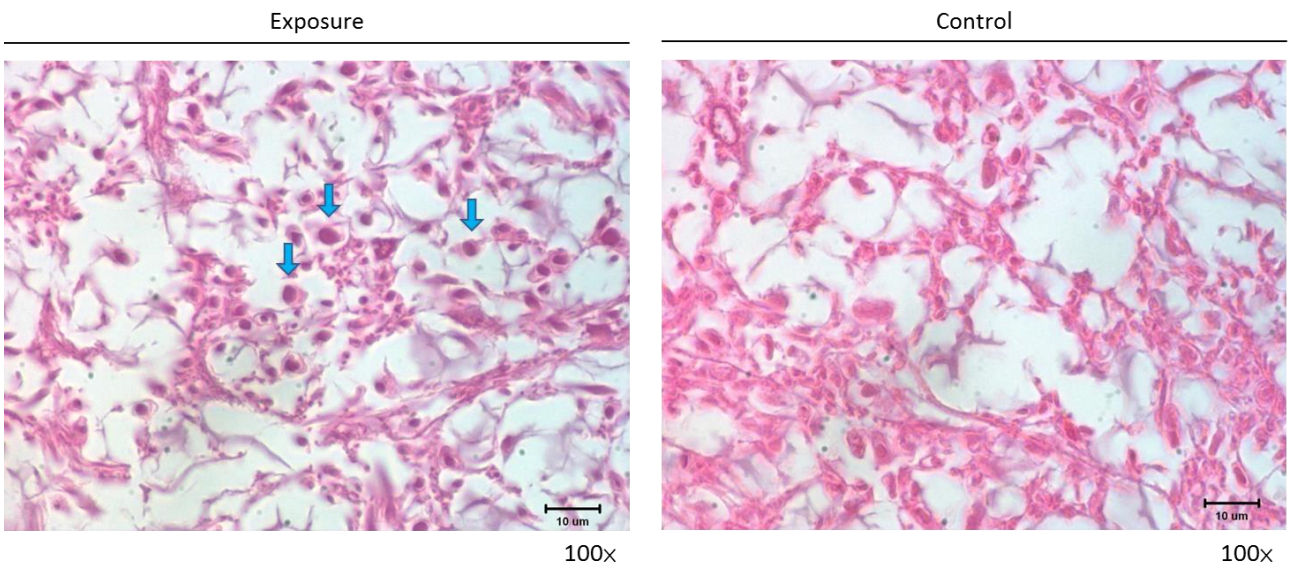

Figure 2 Increased inflammatory cells were seen in the rats exposed to ambient $PM_{2.5}$.

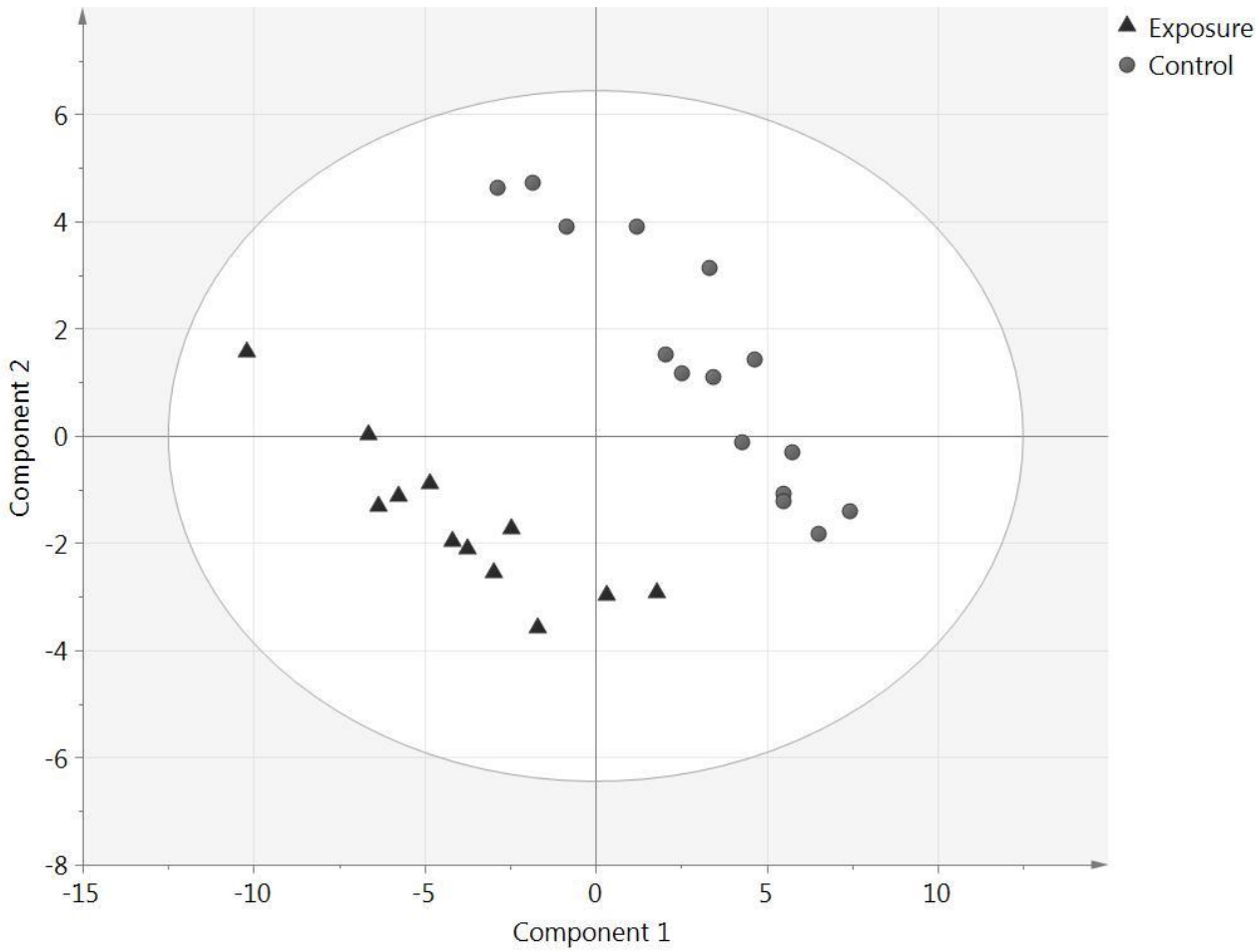

Figure 3 PLS-DA scores scatter plot for three duplicate measurements shows the differentiation between the lipid profile in the exposure (n = 4) and the control (n = 5) group in that the R^2Y and Q^2 were 0.953 and 0.677, respectively.

Tables

Table 1

Significantly changed phosphatidylcholines (PCs) in the rats chronically exposed to ambient $PM_{2.5}$

PC	m/z	Rt	VIP	Fold change [a]
Lyso-PC				
PC(16:0/0:0)	495.7	1.34	1.74	0.70**
PC(18:1/0:0)	521.6	1.39	1.28	0.66**
PC(18:0/0:0)	523.8	1.60	1.05	0.80**
Surfactant PC				
PC(16:0/20:4)	782.0	2.40	1.53	0.86**
PC(18:0/18:1)	788.1	2.96	1.47	0.84**
PC with PUFA				
PC(34:4) [b]	754.0	2.23	1.33	0.62**
PC(16:0/20:4)	782.0	2.40	1.53	0.86**
PC(38:4)	811.6	2.99	1.16	0.82**
PC(18:0/22:4)	838.2	2.80	1.30	0.75**
PC(42:4)	866.3	2.39	1.52	0.83**
PC(44:5)	892.2	2.51	1.01	0.79**
Plasmenylcholine				
PC(O-14:1/16:0)	689.5	2.35	1.07	0.74**
PC(P-16:0/16:0)	718.0	2.79	1.00	0.84**
PC(O-16:0/16:0)	720.0	2.85	1.27	0.78**
PC(O-16:0/18:1)	746.0	2.84	1.17	0.84**

m/z: mass-to-charge ratio; Rt: retention time; VIP: variable importance in projection. PUFA: polyunsaturated fatty acyl chains.

[a] Peak area ratio for the exposure to the control group

[b] PCs identified using LIPID Metabolites and Pathways Strategy structure database were expressed as PC(A:B), where A and B are the sum of number of carbons and unsaturated double bonds, respectively, in the two fatty acyl chains.

**: $p < 0.05$ in Wilcoxon rank sum tests for PC profile comparison between two groups